JOURNAL OF CATALYSIS 129, 402–413 (1991)

Characterization of $RuCu/SiO_2$ Catalysts by Infrared Spectroscopy of Adsorbed Carbon Monoxide

RENBIAO LIU,* BERND TESCHE,† AND HELMUT KNÖZINGER*

*Institut für Physikalische Chemie, Universität München, Sophienstrasse 11, 8000 München 2, Germany; and †Fritz-Haber-Institut der Max-Planck-Gesellschaft, Faradayweg 4-6, 1000 Berlin 33, Germany

Received August 8, 1990; revised December 3, 1990

$RuCu/SiO_2$ catalysts were characterized by temperature-programmed reduction (TPR), transmission electron microscopy (TEM), and IR spectroscopy of adsorbed carbon monoxide. The catalysts contained 5 wt% Ru and varying amounts of Cu up to a maximum atomic ratio Ru : Cu of 1 : 1.6. At this composition accessible Ru sites could not be detected. Model calculations indicated that Ru particles might be encapsulated by one to two atomic layers of Cu at this composition. The CO stretching frequency of adsorbed CO on this material appeared at higher values than it did on pure Cu/SiO_2 which should indicate a charge transfer from Cu to Ru. This conclusion is supported by the CO carbonyl spectra of CO adsorbed on materials containing less Cu. When Ru sites were detected by their characteristic CO stretching bands besides Cu–CO species, the Ru–CO stretching frequency was shifted to lower values as compared to the frequency observed for pure Ru/SiO_2. This is consistent with the suggested charge transfer from Cu to Ru. Experiments with $^{12}CO/^{13}CO$ mixtures indicated that dipole–dipole interactions occur between CO oscillators adsorbed on Ru sites in the bimetallic materials at sufficiently low Cu content. This suggests that the bimetallic particles expose islands of uncovered Ru surface large enough for the dipole–dipole coupling effects to occur.

INTRODUCTION

Ruthenium and copper are immiscible in the bulk. Despite the impossibility of forming binary alloys of these metals, silica-supported binary Cu/Ru catalysts showed characteristic adsorption and catalytic properties which clearly indicated Cu–Ru interactions in these materials (*1–14*). These observations motivated extensive investigations to characterize the geometric structure and electronic properties of these supported bimetallic catalysts (*3–6, 10–14*). Also, numerous surface science studies have been reported on model systems in which Cu was deposited on Ru(0001) single crystal surfaces (*15–26*).

Sinfelt and co-workers (*2, 3*) reported on a Cu-induced suppression of hydrogen chemisorption for silica-supported catalysts; this conclusion is consistent with the structural model of the bimetallic particles consisting of a Ru core encapsulated by a Cu layer, which was developed by Sinfelt and co-workers (*5*) on the basis of EXAFS results. In contrast, Haller and co-workers (*6, 7*) did not find any significant influence of Cu on the hydrogen chemisorption capacity of supported Ru. Depending on the support silica even an increase was observed on addition of Cu (*14*). A suppression of hydrogen chemisorption was also observed on Cu-covered Ru(0001) surfaces by Christmann *et al.* (*15, 16*) and Yates *et al.* (*17*) proposed a site-blocking mechanism by Cu.

Contradictory views exist regarding the electronic interaction between copper and ruthenium. Schoenmaker-Stolk *et al.* (*13*) concluded from their XPS studies of silica-supported Ru–Cu catalysts with low Cu content that an electron transfer from Ru to Cu had occurred. Guo *et al.* (*10*) reported that carbonyl infrared bands of adsorbed CO shifted to lower and higher frequencies, respectively, when bonded to Ru or Cu in bimetallic catalysts as compared to monometallic materials. This result indicates a charge transfer from Cu to Ru, in contrast

0021-9517/91 $3.00

to the conclusions of Schoenmaker-Stolk *et al.* (*13*). Electron transfer from Cu to Ru was also supported by model studies on Cu-covered Ru(0001) faces by Houston *et al.* (*22*). The opposite charge transfer was suggested on the basis of work function measurements by Christmann *et al.* (*15*). This, however, was based on an erroneous data analysis and was later corrected (*27*). Hence, work function changes on deposition of Cu onto Ru(0001) also indicate electron transfer from Cu to Ru.

Recent photoemission studies of adsorbed xenon by Kim *et al.* (*28*) indicated that the distribution of Cu on polycrystalline Ru powder differed from that on Ru single-crystal surfaces. Significant differences in metal distribution are therefore inferred for supported bimetallic catalysts as compared to Cu/Ru(0001) model systems.

Despite the potential of infrared spectroscopy of adsorbed carbon monoxide for probing the nature of metal sites and their electronic state (*29*), surprisingly few investigations of this kind have been published for silica-supported bimetallic Cu/Ru catalysts. As mentioned above, Guo *et al.* (*10*) concluded from their carbonyl IR spectra of chemisorbed CO that a charge transfer from Cu to Ru had occurred in their samples which were prepared by sequential impregnation of the silica support with the two precursors. IR spectra of CO adsorbed on Cu/Ru supported catalysts were also reported by Sixta (*30*) and recently by Hong *et al.* (*14*). In addition, Paul and Hoffmann (*21*) obtained evidence for a metal–metal interaction from their EELS spectra of CO chemisorbed on Cu/Ru(0001) model systems.

The present study was carried out with the goal of exploiting the potential of CO chemisorption in conjunction with IR spectroscopy for the characterization of chemisorption sites and for probing the possible electronic interaction between Cu and Ru as well as the geometric blocking of Ru sites by Cu more extensively. The materials studied were prepared by coimpregnation of both metal precursors, a preparation procedure which was also applied by Sinfelt (*1*) in his early studies. The IR studies were performed over a wide temperature range including adsorption and spectroscopy at low temperature, namely 80 K, and they were complemented by temperature-programmed reduction (TPR) measurements and transmission electron microscopy (TEM) to obtain information on reduction behavior and particle size distributions in dependence on catalyst composition.

EXPERIMENTAL

Materials and Catalyst Preparation

The silica used as a support was Aerosil 200 (Degussa), which had a BET surface area of 200 m^2/g. Supported Ru catalyst precursors were prepared by adding silica to an aqueous solution at pH 7 containing appropriate amounts of ruthenium trichloride (Johnson–Matthey) so as to yield a loading of 5 wt% Ru metal. Typically 6 cm^3 solution were used per gram of silica support. The water was allowed to evaporate with continuous stirring at 363 K in air and the resulting paste was dried at 383 K in air for 16 h. Supported Cu and bimetallic Cu/Ru catalyst precursors were prepared in the same way, the impregnation solution containing either copper nitrate (Fluka) or both ruthenium trichloride and copper nitrate in appropriate concentrations. Nominal loadings and atomic compositions of the prepared materials are summarized in Table 1.

TABLE 1

Composition of CuRu-Bimetallic Catalysts

Sample	Wt% Ru	Wt% Cu	Ru : Cu atomic ratio
5 Ru	5	—	—
5 Cu	—	5	—
5Ru0.1Cu	5	0.1	1 : 0.03
5Ru1Cu	5	1	1 : 0.3
5Ru3Cu	5	3	1 : 1
5Ru5Cu	5	5	1 : 1.6

The gases H_2, O_2, CO, N_2, and He were all Linde products with 99.99% purity. O_2 and H_2O contamination levels in CO, H_2, N_2, and He were further reduced by passing the gases through Oxisorb cartridges. ^{13}CO was from Merck Sharp & Dohme and had an isotopic purity of 99%.

IR Spectroscopy

For IR studies, approximately 60 mg of the dried catalyst precursor material was pressed into thin self-supporting wafers (1.7 × 2.2 cm). The wafers were mounted into a Pt-holder and placed into an *in situ* transmission IR cell, which allowed high-temperature treatments and low-temperature (80–300 K) adsorption and spectroscopy (*31, 32*).

Prior to adsorption of CO, the wafers were evacuated ($<10^{-5}$ mbar) at 383 K for 15 h followed by reduction in flowing H_2 (60 cm^3/min). The sample temperature was raised from room temperature to 623 K in flowing H_2 at a heating rate of 10 K/min and kept at 623 K for 2 h. The wafer was then evacuated at 623 K ($<10^{-5}$ mbar) for 30 min and cooled to the adsorption temperature, i.e., 80 K or 298 K, while continuously pumping.

Infrared spectra were recorded on a Perkin–Elmer 580 B grating spectrometer at a spectral resolution of 3 cm^{-1}. Since computer-based difference spectra could not be recorded, the background absorption of the silica support was eliminated by placing an equivalent pure silica wafer into the reference beam of the spectrometer.

Temperatire-Programmed Reduction (TPR)

Typically 500 mg of the catalyst precursors were placed into an appropriate flow reactor, flushed with dry He (40 cm^3/min) at 298 K for 2 h, and then heated at a constant heating rate of 7 K/min from 298 to 773 K in a He stream containing 11% H_2 (total flow rate: 45 cm^3/min). The gas mixture leaving the reactor was passed through a Pd-diffusion cell (to remove the water vapor from the mixture) and the H_2 consumption was then measured in an N_2 carrier gas in a thermal conductivity detector.

Transmission Electron Microscopy (TEM)

Transmission electron micrographs were taken on a Philips EM 400 T electron microscope at an acceleration voltage of 100 kV and instrumental magnifications between 120,000× and 330,000×. Metal particle size distributions after standard reduction were obtained by counting several hundred particles. The number average diameter was calculated as $d_n = n_i d_i / \Sigma n_i$, where d_n is the average diameter of the particles and n_i the number of particles having diameters in the range ($d_i \pm 0.5$) nm.

RESULTS

Temperature-Programmed Reduction

TPR profiles of the various materials are summarized in Fig. 1. The reduction was completed in all cases at temperatures below 600 K. Additional H_2 consumptions were not observed at higher temperatures up to 773 K.

The reduction profiles of the pure Cu/SiO_2 catalysts show characteristic peak maxima at 519 to 532 K, the position shifting to higher temperature as the metal loading increases. In contrast, the pure Ru/SiO_2 catalyst containing 5 wt% Ru reduces at approximately 100 K lower temperatures. The corresponding reduction profile shows two poorly resolved peak maxima at 420 and 431 K.

The reduction profiles for the bimetallic materials clearly indicate an interaction between the metal precursors on the support surface, since peak maxima (at least at Cu contents greater than 0.1 wt%) are neither characteristic for those of pure Ru nor of pure Cu. As shown in Fig. 1c, the addition of 0.1 wt% Cu (sample 5Ru0.1Cu) does not detectably change the reduction profile as compared to that of pure Ru/SiO_2. On addition of 1 wt% Cu(5Ru1Cu) a reduction peak is produced at 448 K with a shoulder near 430 K. The latter may suggest the formation

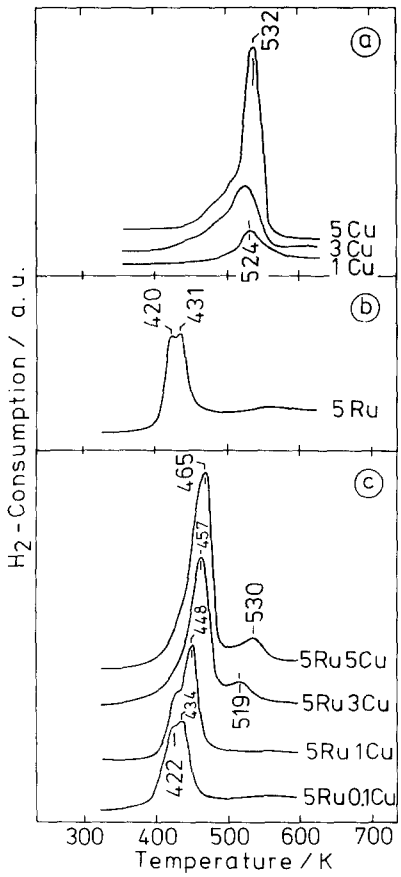

FIG. 1. Temperature-programmed reduction profiles of Cu/SiO$_2$, Ru/SiO$_2$ and CuRu/SiO$_2$ of varying loadings and composition: (a) 5Cu, 3Cu, and 1Cu; (b) 5Ru; (c) 5Ru0.1Cu, 5Ru1Cu, 5Ru3Cu, and 5Ru5Cu.

of pure Ru particles at this Ru : Cu atomic ratio 1 : 0.3. The main peak, however, is clearly shifted to higher temperature and presumably indicates the formation of bimetallic clusters. At still higher Cu contents (samples 5Ru3Cu and 5Ru5Cu), the low-temperature shoulder almost entirely disappears, indicating the absence of significant numbers of monometallic Ru particles. The main peak is further shifted to higher temperatures, namely 457 K for 5Ru3Cu and 465 K for 5Ru5Cu. Moreover, additional reduction peaks appear in the temperature range characteristic for the reduction of the pure Cu precursor, namely 519 and 530 K. This indicates formation of some monometallic Cu particles in addition to the majority bimetallic particles, due to the increased Cu concentration (atomic ratios Ru : Cu equal to 1 : 1 and 1 : 1.6).

Particle Size Distributions

Typical micrographs of the monometallic materials 5Ru and 5Cu after reduction in flowing H_2 at 623 K for 2 h are shown in Fig. 2. It is interesting to note that even at the highest loadings (namely 5 wt%) particles cannot be detected at this magnification for the monometallic 5Cu sample. This may be due to low contrast due to the low atomic number of Cu; it must, however, also indicate a rather high dispersion of metallic Cu in these materials.

In contrast, particles can clearly be detected in the micrograph of 5Ru (see Fig. 2) and the bimetallic materials. Particle size distributions are shown in the histograms of Fig. 3 for samples 5Ru, 5Ru1Cu and 5Ru5Cu. The average particle sizes d_n are also given in the figure. They increase as the Cu content of the samples increases from 1.9 nm for monometallic 5Ru to 2.5 nm for the bimetallic 5Ru5Cu.

Infrared Spectra of Chemisorbed CO

Cu/SiO$_2$. Figure 4 shows a series of carbonyl infrared spectra adsorbed on 5Cu after standard reduction. Three bands are observed at 2153, 2134, and 2114 cm^{-1}. The two bands at higher wavenumbers belong to weakly adsorbed species, since they can be easily removed on evacuation at 80 K and their intensities are strongly reduced at higher temperature under the same CO pressure (see spectrum c in Fig. 4).

The low-frequency band which is observed at 2114 cm^{-1} at 80 K shifts to higher wavenumbers when the CO coverage is reduced under constant CO pressure at increasing temperature; it appears at 2119 cm^{-1} at 115 K and at 2127 cm^{-1} at 298 K. The corresponding species is labile at 298 K since the band can be quantitatively eliminated on evacuation at 298 K.

The bands at 2153 and 2134 cm^{-1} are to

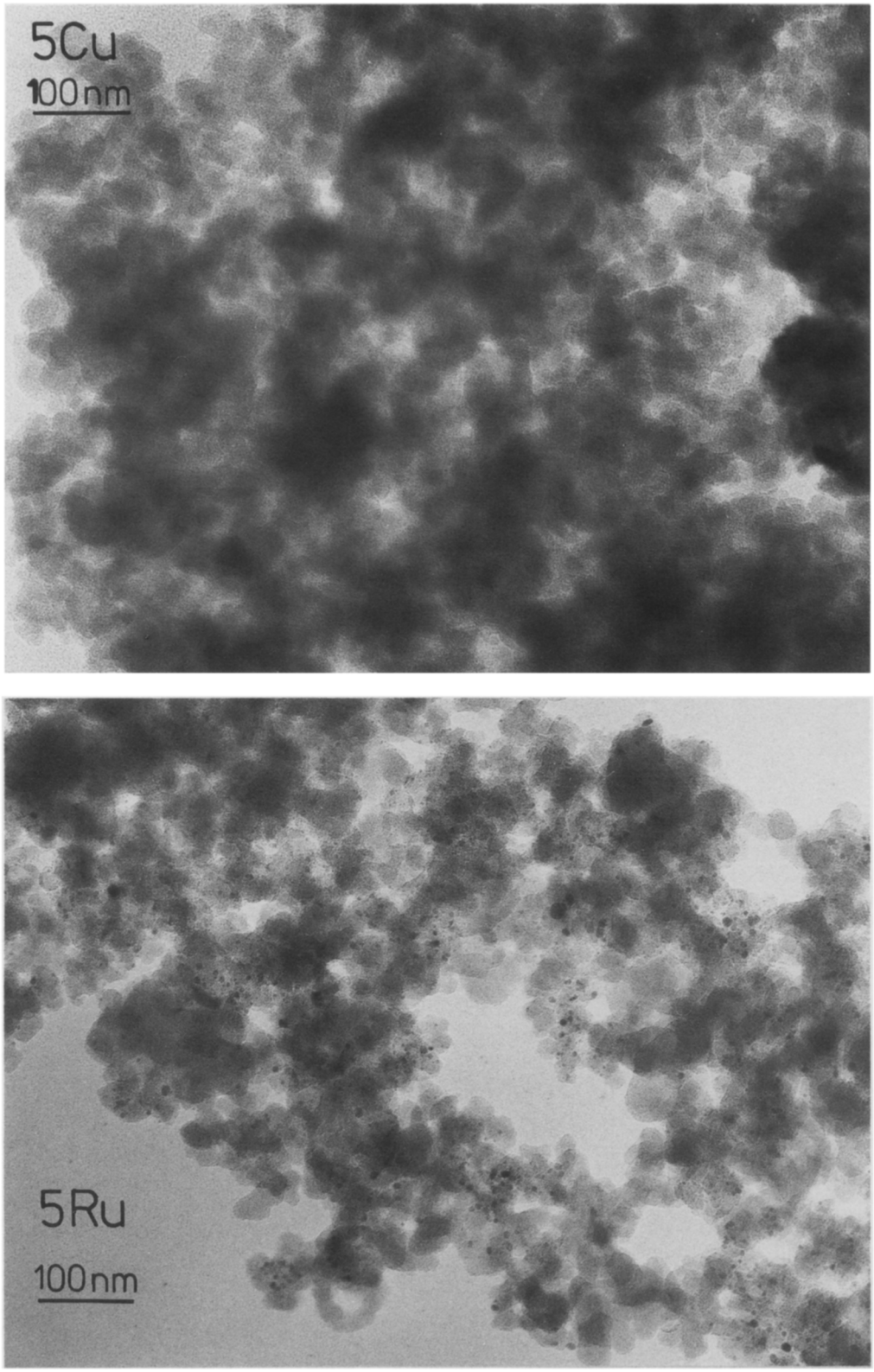

FIG. 2. Transmission electron micrographs of 5Cu and 5Ru after reduction at 623 K for 2 h.

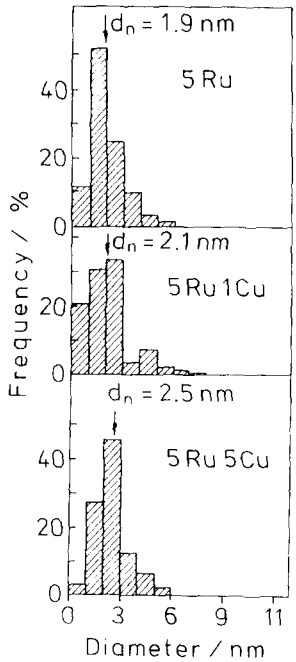

FIG. 3. Metal particle size distributions for 5Ru, 5Ru1Cu, and 5Ru5Cu after reduction at 623 K for 2 h. The number average particle diameters d_n are also given.

be assigned to hydrogen-bonded and physically adsorbed CO (*33, 34*), while the band position at 2114–2127 cm^{-1} and the relative stability of this band are characteristic for CO adsorbed on Cu sites (*29, 35–39*). The frequency shift to higher wavenumber with increasing temperature can be attributed to two effects: first, a particle size effect due to CO being adsorbed more strongly on smaller particles, and second, a coupling effect with lattice vibrations (*40, 41*).

Ru/SiO_2. When CO is adsorbed at 298 K on 5Ru after standard reduction, an asymmetric band centered at 2042 cm^{-1} is observed (Fig. 5, spectrum a). The corresponding species is stable at 298 K and is to be assigned to CO adsorbed on metallic Ru (*29, 42*). Evacuation at 573 K leads to partial desorption and the carbonyl band shifts to 2024 cm^{-1} as the coverage decreases (spectrum b in Fig. 5). This coverage dependence of the carbonyl frequency may indicate dipole–dipole interactions between neighboring adsorbed CO oscillators (*43–50*). $^{12}CO/^{13}CO$ mixtures at constant total pressure and varying isotopic ratios have therefore been adsorbed to test whether in fact this type of lateral interactions is operative. The results are shown in Fig. 5. The spectra clearly show a shift of the carbonyl band from 2042 cm^{-1} to lower values as the ^{13}CO partial pressure is increased relative to that of ^{12}CO, consistent with the assumption of dipole–dipole coupling. As pure ^{13}CO is adsorbed a broad band at 1997 cm^{-1} is observed (spectrum h in Fig. 5) which is consistent with the expected isotope shift (calculated value 1997 cm^{-1}). The width of this band as it appears in the figure is apparent since the wavenumber scale is expanded by a factor of two below 2000 cm^{-1} relative to that above 2000 cm^{-1}.

Bimetallic catalysts. Figure 6 shows spectra of CO adsorbed on 5Ru5Cu (atomic ratio

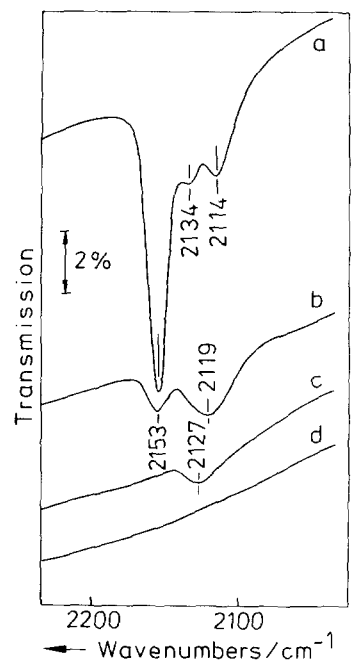

FIG. 4. Infrared spectra of ^{12}CO adsorbed on 5Cu after reduction at 623 K for 2 h. (a) 53 mbar CO at 80 K; (b) 53 mbar CO at 115 K; (c) 53 mbar CO at 295 K; and (d) after evacuation at 295 K for 1 min.

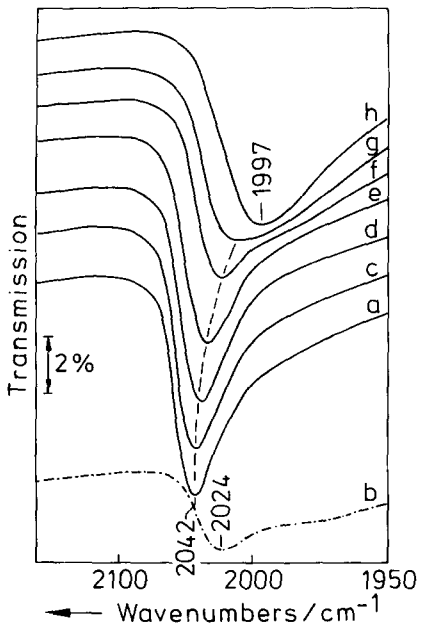

FIG. 5. Infrared spectra of ^{12}CO and $^{12}CO/^{13}CO$ isotopic mixtures adsorbed on 5Ru (reduction at 623 K for 2 h). A total equilibrium carbon monoxide pressure of 53 mbar was applied at 295 K. (a) 100% ^{12}CO; (b) after evacuation at 573 K for 5 min.; (c) 12,5% ^{13}CO; (d) 25% ^{13}CO; (e) 50% ^{13}CO; (f) 75% ^{13}CO; (g) 87,5% ^{13}CO; and (h) 100% ^{13}CO.

Ru:Cu = 1:1.6). At 80 K bands at 2155 cm^{-1} (hydrogen-bonded species) and at 2123 cm^{-1} are observed, while the only detectable band at 298 K is that at 2127 cm^{-1}. This band is easily eliminated on evacuation at 298 K. Position and lability of this band are characteristic for CO adsorbed on Cu (see Fig. 4), whereas no bands can be detected in the wavenumber range which is typical for CO on Ru below 2100 cm^{-1}. It thus appears that Ru sites remain inaccessible to CO in sample 5Ru5Cu.

When the Cu content is reduced as in samples 5Ru3Cu (Ru:Cu = 1:1) and 5Ru1Cu (Ru:Cu = 1:0.3), contributions from CO adsorbed on Ru sites appear in the spectra. Figure 7, spectrum a, shows carbonyl spectra of CO adsorbed on 5Ru3Cu at 298 K. At 53 mbar CO two bands are seen at 2138 and 2034 cm^{-1} in the Cu and Ru regions, respectively. After exposing the sample to 53 mbar CO at 573 K for 10 min the spectra taken at 298 K show these bands at 2144 and 2035 cm^{-1} (spectrum b in Fig. 7). Similarly, these bands appear at 2141 and 2035 cm^{-1} on sample 5Ru1Cu and 2144 and 2035 cm^{-1} on sample 5Ru0.1Cu with increasing relative intensities for the low-frequency band (CO on Ru) as the Cu content is decreased.

The assignment of the band at 2144 cm^{-1} to a Cu–CO complex and of that at 2035 cm^{-1} to Ru–CO can be supported by the spectral characteristics observed when $^{13}CO/^{12}CO$ mixtures are adsorbed at varying isotopic compositions. Figure 8 shows a series of spectra at beam temperature of $^{13}CO/^{12}CO$ mixtures adsorbed on 5Ru3Cu at constant total pressure of 53 mbar. The characteristic bands at 2144 and 2035 cm^{-1} are seen in pure ^{12}CO (spectrum a). The high-frequency band at 2144 cm^{-1} is reduced in intensity as the $^{13}CO/^{12}CO$ ratio is increased while a new band at 2094 cm^{-1} develops. This band must be attributed to the isotopically shifted carbonyl stretching mode, the calculated band position being 2096 cm^{-1}. The positions of these two bands remain

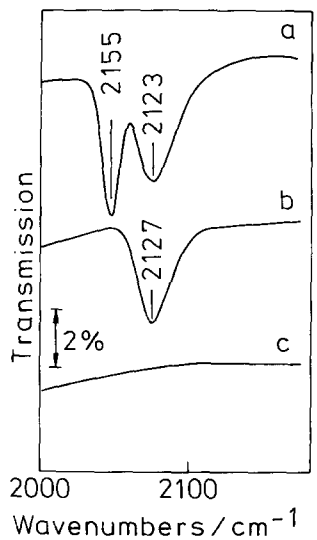

FIG. 6. Infrared spectra of ^{12}CO adsorbed on 5Ru5Cu after reduction at 623 K for 2 h. (a) 53 mbar CO at 80 K; (b) 53 mbar CO at 295 K; and (c) after evacuation at 295 K for 5 min.

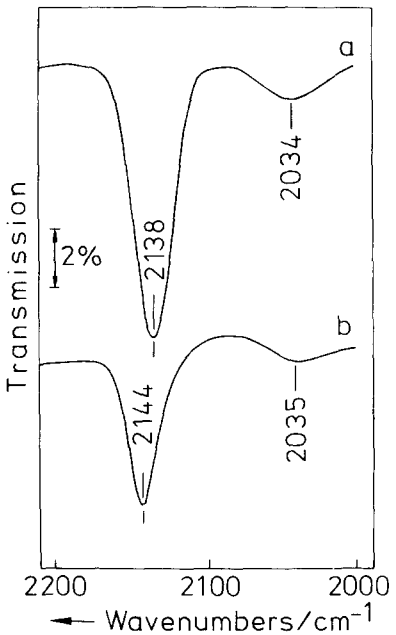

FIG. 7. Infrared spectra of ^{12}CO adsorbed on 5Ru3Cu after reduction at 623 K for 2 h. (a) 53 mbar CO at 295 K; and (b) after treatment of the catalyst in CO at 573 K for 10 min. Spectrum taken at 295 K.

remarkably constant at 2144 and 2094 cm^{-1} as the isotopic composition of the adsorbate is varied. This behavior has been reported as characteristic for CO adsorbed on Cu (*51*), thus supporting the assignment of the 2144 cm^{-1} in bimetallic catalysts to Cu–CO species.

The relatively weak band at 2035 cm^{-1} (spectrum a, Fig. 8) which is assigned as a terminal Ru–^{12}CO species clearly shifts to lower frequencies with increasing $^{13}CO/^{12}CO$ isotopic ratio, while there seems to be very little intensity in the Ru–^{13}CO range below 2000 cm^{-1}. Both phenomena, the dependence of carbonyl band positions on isotopic composition and the low intensities of the low-frequency component (intensity stealing into the high-frequency band), are well known for CO adsorbed on Group VIII metals (*52, 53*).

These trends can obviously be observed more clearly for samples containing lower Cu content. This is shown for 5Ru1Cu in Fig. 9. The behavior of the bands at 2141 and 2092 cm^{-1} is identical to that observed for sample 5Ru3Cu in Fig. 8. The shift of the Ru–^{12}CO band to lower frequency with increasing $^{13}CO/^{12}CO$ isotopic ratio is clearly evident. Also, the intensity stealing from the low-frequency Ru–^{13}CO species is obvious, e.g., from the fact that in a 50 : 50 isotopic mixture (spectrum c in Fig. 9) an intense Ru–^{12}CO band at 2021 cm^{-1} is seen while the presence of Ru–^{13}CO species is only indicated by a broad shoulder toward lower frequencies.

DISCUSSION

The TPR experiments with bimetallic materials clearly indicated an interaction between the Ru and Cu precursor salts, since

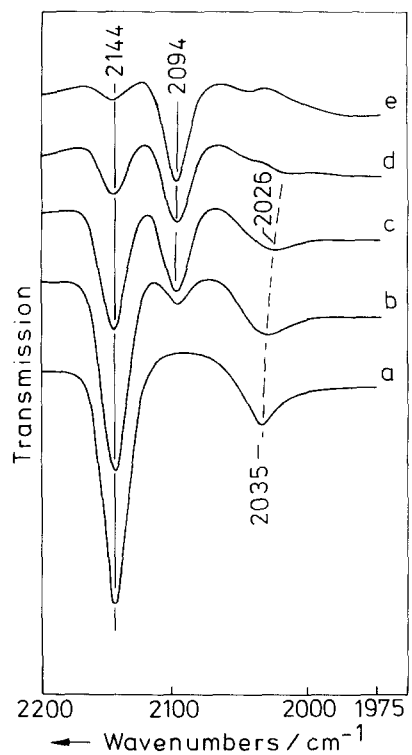

FIG. 8. Infrared spectra of ^{12}CO and $^{12}CO/^{13}CO$ isotopic mixtures adsorbed on 5Ru3Cu (reduction at 623 K for 2 h). A total equilibrium carbon monoxide pressure of 53 mbar was applied at 573 K for 10 min prior to recording the spectra at 295 K: (a) 100% ^{12}CO; (b) 15% ^{13}CO; (c) 50% ^{13}CO; (d) 65% ^{13}CO; and (e) 87,5% ^{13}CO.

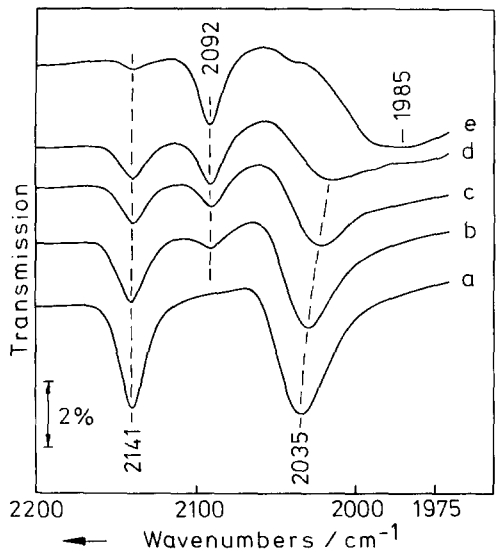

FIG. 9. Infrared spectra of ^{12}CO and $^{12}CO/^{13}CO$ isotopic mixtures adsorbed on 5Ru1Cu (reduction at 623 K for 2 h). A total equilibrium carbon monoxide pressure of 53 mbar was applied at 295 K: (a) 100% ^{12}CO; (b) 25% ^{13}CO; (c) 50% ^{13}CO; (d) 65% ^{13}CO; and (e) 95% ^{13}CO.

both were reduced simultaneously at an intermediate temperature regime between 450 and 465 K when the Cu content was equal to or higher than 1 wt%. In contrast, the pure Ru precursor was reduced at 430 K and the pure Cu precursor (depending on loading) between 520 and 530 K (see Fig. 1). Only at the lowest Cu contents, i.e., in samples 5Ru0.1Cu and 5Ru1Cu, can reduction of noninteracting Ru species be detected as a shoulder at 430 and 422 K, respectively. Rather small relative contributions of noninteracting Cu species were evident in samples 5Ru3Cu and 5Ru5Cu (see Fig. 1). The respective peaks at 519 and 530 K correspond to approximately 12% of the total hydrogen consumption. We therefore conclude that at least for the two samples 5Ru3Cu and 5Ru5Cu (Ru : Cu atomic ratios of 1 : 1 and 1 : 1.6) the majority of particles formed during the standard reduction are bimetallic. Pure Ru particles are presumably present in only very small number and pure Cu particles, although detectable in TPR spectra, should also remain at low abundance.

Bond and Xu (*11*) had suggested that the direct reduction of a dried catalyst precursor without any calcination should lead to highly dispersed bimetallic particles. They reported that $RuCl_3$ species would begin to reduce in H_2 and form metal particles near 400 K. Dissociative chemisorption of H_2 would then lead to reduction of Cu^{2+} via hydrogen spillover and bimetallic particles would form in H_2 at temperatures below 620 K. The reduction procedure applied in the present study was very similar to that described above.

As a matter of fact, highly disperse reduced metal particles were formed in our materials. The average particle size in sample 5Ru5Cu was estimated to be 2.5 nm as compared to 1.9 nm for the pure Ru catalyst 5Ru. Bond and Xu (*11*) described their bimetallic particles as consisting of a Ru core which was encapsulated by a Cu coat. If we assume identical numbers of spherical metal particles in both 5Ru and 5Ru5Cu and equal composition for all bimetallic particles in 5Ru5Cu, we can estimate the theoretical average particle size in the bimetallic catalyst provided the "cherry" model as described above is valid. The Ru core would then have an average diameter d_n = 1.9 nm and the addition of Cu at an atomic ratio Ru : Cu = 1.6 would create spherical bimetallic particles with an average diameter d_n = 2.54 nm which corresponds to a uniform Cu coat thickness of 0.3 nm. This theoretical average particle diameter (which is based on a certainly hypothetical model) is surprisingly close to that found experimentally by TEM, namely 2.5 nm. Even though the assumptions made are unrealistic, this estimate nevertheless indicates that the amount of Cu in 5Ru5Cu is sufficient to totally encapsulate the Ru particles. The coat thickness of 0.3 nm would correspond to one to two atomic layers. Hence, it is to be expected that Cu in this material can entirely block CO adsorption on Ru. However, with a coat thickness corresponding to only one or two

atomic layers, it should be possible to probe the electronic state of the Cu sites by CO if there were an electronic interaction between Cu and Ru.

The blocking effect of Cu for the CO adsorption on Ru is evident from the IR carbonyl spectra (Fig. 6 and 7). The intensity of the Ru–^{12}CO species in the wavenumber range below 2050 cm^{-1} is continuously attenuated as the Ru : Cu atomic ratio decreases. As predicted above on the basis of the hypothetical model, no Ru–^{12}CO bands are detectable for 5Ru5Cu (see Fig. 6). This indicates that accessible Ru surface is no longer exposed at this composition.

Most interestingly, the frequencies of Cu–^{12}CO species are shifted to higher values for the bimetallic materials as compared to pure silica-supported Cu. There seems to be a high-frequency limit at 2144 cm^{-1} for materials having low Cu content in which free Ru surface is still exposed. With increasing Cu content, this frequency decreases and seems to approach the value for pure Cu (2114 cm^{-1}) at 80 K (see Fig. 4), when the proposed Cu coat becomes thicker. In sample 5Ru5Cu the corresponding frequency was observed at 2123 cm^{-1} (see Fig. 6). These high carbonyl frequencies indicate a positive polarization of the Cu sites as reported earlier by Guo *et al.* (*10*). The slightly higher thermal stability of the CO species on the bimetallic catalyst as compared to the pure Cu is consistent with the assumption of a positively charged adsorption site. Frequencies near 2130 cm^{-1} have been reported for Cu^+–CO complexes in supported oxide systems (*35, 54*). It is not, however, implied that the bimetallic catalysts contain Cu in the formal oxidation state 1+. Rather the Cu layers do in fact have metallic character as indicated by the effects of lateral interactions between adsorbed CO molecules on the IR spectra. The fact that the Cu–^{12}CO and Cu–^{13}CO frequencies remain constant with variations of isotopic composition is due to a compensation of two effects, namely a positive frequency shift caused by dipole–dipole coupling and a negative frequency shift due to a chemical inductive effect (*51*). The coupling becomes evident from a small intensity stealing into the high-frequency Cu–^{12}CO band which can be seen in Figs. 8 and 9. It is thus inferred that the positive polarization of the Cu overlayer is due to a charge transfer from Cu to Ru in agreement with the conclusions of Guo *et al.* (*10*).

As a consequence of this charge transfer, the CO frequencies observed for Ru–CO species do in fact shift to lower wavenumbers on addition of Cu as compared to the band position at 2042 cm^{-1} on pure 5Ru. The Ru–^{12}CO band is observed near 2035 cm^{-1} on 5Ru1Ru and 5Ru3Cu. This shift to lower frequency can be explained by an enhanced π-back-donation due to the increased electron density at Ru sites which is brought about by the charge transfer from Cu. It has been shown in Figs. 8 and 9 that dipole–dipole coupling between Ru–CO oscillators occurs on materials with partial coverage of the Ru particles by Cu. This is observed even for 5Ru3Cu although in this sample with a Ru : Cu atomic ratio of one, only a small portion of the total Ru should be exposed. This can be explained in either of two ways. First, a small number of Ru particles may have remained uncovered by Cu. Second, Cu is located on the surface of all particles in the form of islands. This would presumably leave sufficiently large patches of exposed Ru surface so that dipole–dipole coupling effects could occur between adsorbed Ru–CO species. This model would also account for the relatively small frequency shift for Ru–CO species and its independence of the Cu content since the electronic effects should act only over short distances.

The site blocking effect of Cu for CO adsorption on Ru has also been reported by Sakakini *et al.* (*24*) for the Cu/Ru(0001) system. These authors also reported on evidence from static SIMS for the induction of bridge-bonded Ru_2CO species and on bridging CO species RuCuCO on mixed metal sites with specimens having submonolayer

Cu coverage. Despite the low inherent spectral resolution of EELS, the same authors (*24*) believe to have seen evidence for these adsorbed CO species also in their electron loss spectra. No indication for the formation of bridging CO species could be obtained in the present study of the silica-supported bimetallic catalysts. Admittedly this may be due to the relatively poor spectral quality in the frequency regime below 1900 cm^{-1}, where Si–O overtone and combination bands strongly interfere with the spectra of adsorbed species. However, in agreement with the present results, Sakakini *et al.* (*24*) also interpret experimental frequency shifts for Cu–CO and Ru–CO species in the bimetallic system relative to the carbonyl frequencies observed for the pure metals as being due to an electronic interaction between the two metals.

A charge transfer from Cu to Ru in bimetallic particles supported on silica is clearly implied by the present results, in agreement with earlier IR studies (*10*), in contrast, however, to the XPS results reported by Schoenmaker-Stolk *et al.* (*13*). This conclusion is also in line with model studies of Cu overlayers on Ru(0001) single-crystal faces by Houston *et al.* (*22*). The discrepancy with the work function measurements by Christmann *et al.* (*15*) is only apparent and the corrected interpretation of Ertl (*27*) in fact also suggests the charge transfer occurs from Cu to Ru. The IR data reported here are also consistent with an encapsulation of Ru particles by Cu, a model which was first suggested by Sinfelt and co-workers (*1–5*) and also proposed by others, e.g., Bond and Xu (*11*) as discussed above.

ACKNOWLEDGMENTS

This research was financially supported by the Deutsche Forschungsgemeinschaft and the Fonds der Chemischen Industrie. A grant from the Max-Buchner-Forschungsstiftung and a loan of ruthenium chloride from Johnson–Matthey are gratefully acknowledged.

REFERENCES

1. Sinfelt, J. H., *J. Catal.* **29,** 308 (1973).
2. Sinfelt, J. H., La, Y. L., Cusumano, J. A., and Barnett, A. E., *J. Catal.* **42,** 227 (1976).
3. Prestridge, E. B., Via, G. H., and Sinfelt, J. H., *J. Catal.* **50,** 115 (1977).
4. Helms, C. R., and Sinfelt, J. H., *Surf. Sci.* **72,** 229 (1978).
5. Sinfelt, J. H., Via, G. H., and Lytle, F. W., *J. Chem. Phys.* **72,** 4832 (1980).
6. Rouco, A. J., Haller, G. L., Oliver, J. A., and Kemball, C., *J. Catal.* **84,** 297 (1983).
7. Haller, G. L., Resasco, D. E., and Wang, J., *J. Catal.* **84,** 477 (1983).
8. Hong, A. J., Rouco, A. J., Resasco, D. E., and Haller, G. L., *J. Phys. Chem.* **91,** 2665 (1987).
9. Damiani, D. E., Millán, E. D. P., and Rouco, A. J., *J. Catal.* **101,** 162 (1986).
10. Guo, X., Xin, Q., Li, Y., Jin, D., and Ying, P., *in* "Proceedings, 8th International Congress on Catalysis, Berlin, 1984," Vol. IV, p. 599. Dechema, Frankfurt-am-Main, 1984.
11. Bond, G. C., and Xu, Y. *J. Mol. Catal.* **25,** 141 (1984).
12. Shastri, A. G., Schwank, J., and Galvagno, S., *J. Catal.* **100,** 446 (1986); and references therein.
13. Schoenmaker-Stolk, M. C., Verwijs, J. W., and Scholten, J. J. F., *Appl. Catal.* **30,** 339 (1987).
14. Hong, A. J., McHugh, B. J., Bonneviot, L., Resasco, D. L., Weber, R. S., and Haller, G. L., *in* "Proceedings, 9th International Congress on Catalysis, Calgary, 1988" (M. J. Phillips and M. Ternan, Eds.), Vol. 3, p. 1198. Chem. Institute of Canada, Ottawa, 1988.
15. Christmann, K., Ertl, G., and Shimizu, H., *J. Catal.* **61,** 397 (1980); *Thin Solid Films* **57,** 247 (1979).
16. Christmann, K., and Ertl, G., *J. Mol. Catal.* **25,** 31 (1984).
17. Yates, J. T., Peden, C. H. F., and Goodman, D. W., *J. Catal.* **94,** 321 (1985).
18. Houston, J. E., Peden, C. H. F., Blair, D. S., and Goodman, D. W., *Surf. Sci.* **167,** 427 (1986).
19. Houston, J. E., Peden, C. H. F., Feibelman, P. J., and Hamann, D. R., *Phys. Rev. Lett.* **56,** 375 (1986).
20. Peden, C. H. F., and Goodman, D. W., *J. Catal.* **100,** 520 (1986).
21. Paul, J., and Hoffman, F. M., *Surf. Sci.* **172,** 151 (1986).
22. Houston, J. E., Peden, C. H. F., and Feibelman, P. J., *Surf. Sci.* **192,** 457 (1987).
23. Goodman, D. W., and Peden, C. H. F., *J. Chem. Soc. Faraday Trans. 1* **83,** 1967 (1987).
24. Sakakini, B., Swift, A. J., Vickerman, J. C., Harendt, C., and Christmann, K., *J. Chem. Soc. Faraday Trans. 1* **83,** 1975 (1987).
25. Hoffman, F. M., and Paul, J., *J. Chem. Phys.* **86,** 2990 (1987).
26. Hoffman, F. M., and Paul, J., *J. Chem. Phys.* **87,** 1857 (1987).
27. Ertl, G., private communication.

28. Kim, K. S., Sinfelt, J. H., Eder, S., Markert, K., and Wandelt, K., *J. Phys. Chem.* **91,** 2337 (1987).
29. Sheppard, N., and Nguyen, T. T., *Adv. Infrared Raman Spectrosc.* **5,** 67 (1978).
30. Sixta, H., Doctoral thesis, Universität Innsbruck, 1981.
31. Knözinger, H., Stolz, H., Bühl, H., Clement, G., and Meye, W., *Chem. Ing. Tech.* **42,** 548 (1970).
32. Kunzmann, G., Doctoral thesis, Universität München, 1987.
33. Beebe, T. P., Gelin, P., and Yates, J. T., *Surf. Sci.* **148,** 526 (1984).
34. Zaki, M. I., and Knözinger, H., *Mater. Chem. Phys.* **17,** 201 (1987).
35. Ghiotti, G., Boccuzzi, F., and Chiorino, A., *in* "Adsorption and Catalysis on Oxide Surfaces" (M. Che and G. C. Bond, Eds.), p. 235. Elsevier, Amsterdam, 1985.
36. de Jong, K. P., Geus, J. W., and Joziasse, J., *Appl. Surf. Sci.* **6,** 273 (1980).
37. Kazusaka, A., Yamazaki, A., and Kakuta, V., *J. Chem. Soc. Faraday Trans. 1* **82,** 1553 (1986).
38. Pritchard, J., *Trans. Faraday Soc.* **66,** 427 (1970).
39. Chen, H., White, J. M., and Ekerdt, J. G., *J. Catal.* **99,** 293 (1986).
40. Sheppard, N., *in* "Vibrational Spectroscopy of Adsorbates" (R. F. Willis, Ed.), p. 165. Springer, Berlin, 1980.
41. Castro, G. R., Tacconi, P., Severino, F., and Laine, J., *in* "Lectures on Surface Science" (G. R. Castro and M. Cardona, Eds.), Proc. 4th Lat.-Am. Symp. p. 278. Springer, Berlin, 1987.
42. Solymosi, F., and Raskó, J., *J. Catal.* **115,** 107 (1989).
43. Hammaker, R. M., Francis, S. A., and Eischens, R. P., *Spectrochim. Acta* **21,** 1295 (1965).
44. Shigeishi, R., and King, D. A., *Surf. Sci.* **58,** 379 (1976).
45. Crossley, A., and King, D. A., *Surf. Sci.* **68,** 528 (1977).
46. Haman, G. D., and Lucas, A. A., *J. Chem. Phys.* **68,** 1344 (1978).
47. Greenler, R. G., Leibsler, F. M., and Sorbello, R. S., *J. Electron Spectrosc. Relat. Phenom.* **39,** 195 (1966).
48. Stoop, F., Toolenaar, F. J. C. M., and Ponec, V., *J. Catal.* **73,** 50 (1982).
49. Toolenaar, F. J. C. M., Stoop, F., and Ponec, V., *J. Catal.* **82,** 1 (1983).
50. Hendrickx, H. A. C. M., Bouvrie, C., and Ponec, V., *J. Catal.* **109,** 120 (1988).
51. Hollins, P., and Pritchard, J., *in* "Vibrational Spectroscopy of Adsorbates" (R. F. Willis, Ed.), p. 125. Springer, Berlin, 1980.
52. King, D. A., *in* "Vibrational Spectroscopy of Adsorbates" (R. F. Willis, Ed.), p. 179. Springer, Berlin, 1980.
53. Willis, R. F., Lucas, A. A., and Mahan, G. D., *in* "Chemical Physics of Solid Surfaces and Heterogeneous Catalysts" (D. A. King and D. P. Woodruff, Eds.), Vol. 2, p. 59. Elsevier, Amsterdam, 1983.
54. Kasal, P. H., Bishop, Jr., R. J., and McLeod, Jr., D., *J. Phys. Chem.* **82,** 279 (1987).
55. Vickerman, J. C., Christmann, K., and Ertl, G., *J. Catal.* **71,** 175 (1981).